Chapter 11
Molecular Mechanisms in the Thermochemical Conversion of Lignins into Bio-Oil/Chemicals and Biofuels

Haruo Kawamoto

11.1 Introduction

Lignin accounts for 20–30 % by weight of lignocellulosic biomass, and is a promising renewable resource for the production of aromatic chemicals and bio-fuels [1]. It is composed of phenylpropane units containing three different aromatic ring substitution patterns: *p*-hydroxyphenyl (H), guaiacyl (4-hydroxy-3-methoxyphenyl, G) and syringyl (3,5-dimethoxy-4-hydroxyphenyl, S) [1]. Softwoods contain a greater proportion of G units and smaller amounts of the H type, whereas hardwoods consist of G and S units while herbaceous species contain G, S and H units [1]. These monomers are linked together through ether (C–O) and condensed (C–C) bonds. Accordingly, lignin pyrolysis proceeds heterogeneously, depending on the plant species. This is in contrast to the pyrolysis of cellulose, a homogeneous polymer of D-glucose units connected via β-1 → 4 linkages.

In this chapter, molecular mechanisms involved in lignin pyrolysis are discussed with the focus being primarily on G-lignin after the brief analysis of the devolatilization temperature of lignin and the product compositions. Although many papers have reported theoretical investigations of specific pyrolysis reactions of lignins, this chapter concentrates on the results of experimental investigations conducted by the author's research group.

H. Kawamoto (✉)
Graduate School of Energy Science, Kyoto University,
Yoshida-honmachi, Sakyo-ku, Kyoto 606-8501, Japan
e-mail: kawamoto@energy.kyoto-u.ac.jp

Z. Fang, R.L. Smith, Jr. (eds.), *Production of Biofuels and Chemicals from Lignin*, Biofuels and Biorefineries 6, DOI 10.1007/978-981-10-1965-4_11

11.2 Lignin Devolatilization Temperature

The devolatilization behavior of lignins during pyrolysis has been studied based on thermogravimetric (TG) analyses of lignins isolated from lignocellulosic biomasses [2–5]. Figure 11.1 presents TG and derivative thermogravimetric (DTG) data obtained from milled wood lignin (MWL) isolated from Japanese cedar (*Cryptmeria japonica*), a softwood [6]. Generally, the mass loss of lignins starts at approximately 200 °C, a temperature that is below those associated with the pyrolysis of cellulose and hemicellulose, and the major mass loss is observed between 200 and 400 °C, representing the primary pyrolysis step. Nuclear magnetic resonance (NMR) [4] and model compound [7–11] studies have confirmed that the ether linkages between the phenylpropane units are cleaved in this temperature range. In the case of hardwood lignins consisting of G and S units, the DTG peaks are shifted to slightly lower temperatures (compare 353 °C for Japanese cedar, a softwood, to 326 °C for Japanese beech, a hardwood) [6]. Although the mechanisms responsible for this difference are not presently known, several papers report similar relations [5, 12–14]. The lignin preparation methods are also reported to affect the devolatilization behavior [15].

In the higher temperature range of 400–800 °C, the mass loss rates are reduced and a relatively large amount of residue remains even at 800 °C, a much greater amount than is observed during the pyrolysis of cellulose or hemicellulose. In general, softwood lignins tend to generate larger amounts of residue than hardwood

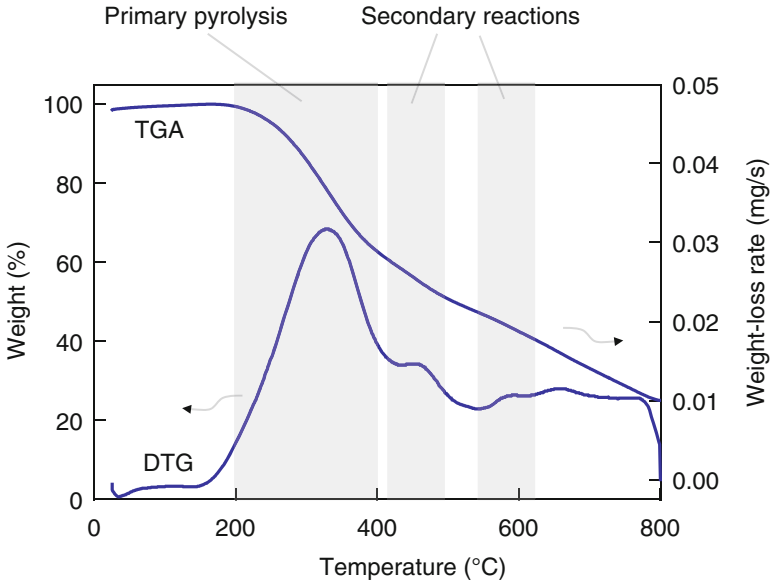

Fig. 11.1 Thermogravimetric analysis of milled wood lignin isolated from Japanese cedar (*Cryptmeria japonica*) (Adapted with permission from Ref. [6], Copyright © 2011 Elsevier)

lignins [3, 12]. This is explained by the greater proportion of condensed type linkages in softwood lignins, which preferentially consist of G units, because these condensed structures are relatively resistant to pyrolytic depolymerization. The C5 positions of the guaiacyl units are involved in the formation of various condensed linkages, such as the 5-5′ and β-5′ types, during lignin biosynthesis, whereas increasing proportions of syringyl units, in which the C5 positions are already substituted by methoxyl groups, makes the contributions of the condensed-type linkages less important.

Even in the high temperature region, several DTG peaks are observed, at approximately 450, 550–600 and 650 °C. These peaks suggest that various temperature-dependent secondary reactions take place upon increasing the pyrolysis temperature. While the TG/DTG plots directly reflect the solid/liquid phase pyrolytic reactions, similar reactions are also considered to proceed in the gas phase, as discussed in Sect. 11.5. Based on the gas phase reactions, these DTG peaks are believed to result from reactions initiated by the homolytic cleavage of the methoxyl C–O bonds and side-chain C–C bonds (at 450 °C) as well as the decomposition of aromatic rings (at 550–600 °C).

11.3 Pyrolysis Products and Effects of Temperature

The chemical structures of the volatile products obtained from lignins have been determined on the basis of gas chromatography/mass spectrometry (GC/MS) [16–18], NMR [4, 18–23] and infrared (IR) [2, 11, 20, 24] analyses of the pyrolysis products from wood and isolated lignin fractions. In addition, other studies have employed pyrolysis directly coupled with GC/MS [25–29] and IR [2, 14] analyses (Py-GC/MS, Py-IR). The volatile products from the pyrolysis of lignins have been found to include aromatic compounds (phenols and aromatic hydrocarbons), low molecular weight (MW) aliphatic compounds (formaldehyde, formic acid, methanol and others) and non-condensable gases such as methane, CO, CO_2 and H_2.

Figure 11.2 summarizes the changes in the aromatic ring and side-chain structures of the GC/MS-detectable products derived from G-type lignin during the pyrolysis of Japanese cedar MWL, under N_2 in a closed ampoule in a furnace preheated to 600 °C [18]. In this pyrolysis system, the temperature inside the ampoule reached 600 °C in 120 s [30], and hence these data show the structural changes of the volatile pyrolysis products as the sample is heated to the pyrolysis temperature.

At 40 s (450 °C) and 60 s (530 °C) points (Fig. 11.2), where the values in parentheses are the associated temperatures, the only aromatic ring in the pyrolysis products is guaiacol (2-methoxyphenol), which is the original repeating unit in the Japanese cedar lignin. In the early stage (40 s) of the pyrolysis (corresponding to the DTG peak at 350 °C), the side chains are primarily unsaturated alkyl (>C=C<, >C=O and conjugated >C=O) groups. The major volatile products in this stage include coniferyl alcohol (R: –CH=CH–CH_2OH), coniferyl aldehyde (R: –CH=CH–CHO), isoeugenol (R: –CH=CH–CH_3), 4-vinylguaiacol (R: –CH=CH_2), vanillin (R:

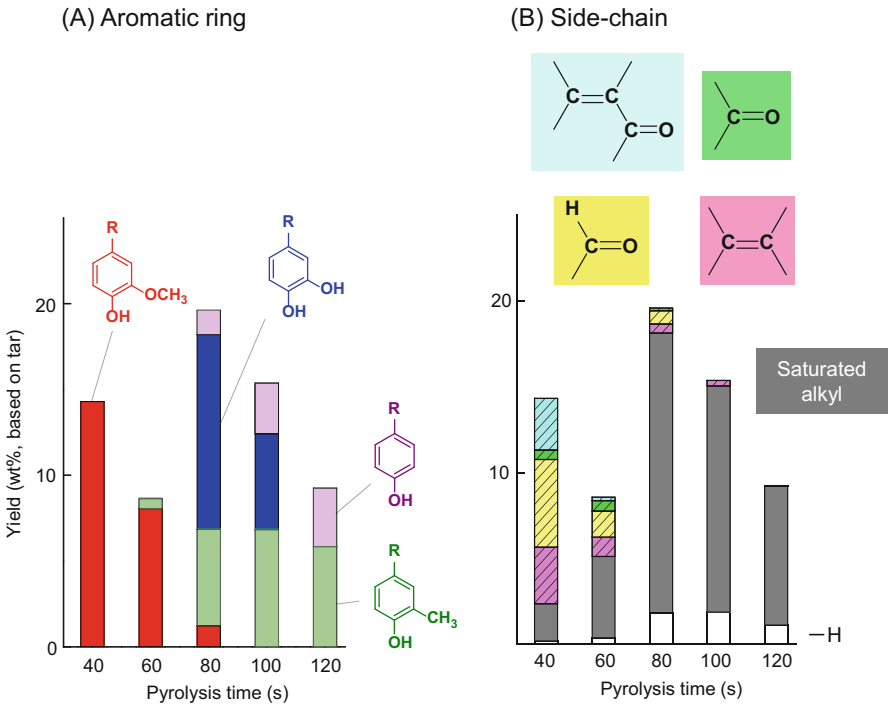

Fig. 11.2 Changes in the aromatic ring and side chain structures of the GC/MS-detectable volatile products from Japanese cedar (*Cryptmeria japonica*) MWL during pyrolysis in a closed ampoule (under N_2) in a furnace preheated to 600 °C. Here pyrolysis time is defined as the total time span over which the ampule is in the furnace (Adapted with permission from Ref. [18], Copyright © 2008 Elsevier)

–CHO) and acetovanillone (R: –CO–CH_3). The unsaturated alkyl side chains gradually transition to saturated alkyls (methyl, ethyl, propyl, 3-hydroxypropyl and others) and non-substituted (–H) types upon increasing the pyrolysis time and temperature. S-lignin is found to generate the corresponding syringol (2,6-dimethoxyphenol) derivatives. These primary products undergo re-polymerization and side chain conversions, as discussed in Sect. 11.4.4, and this re-polymerization reduces the yields of volatile products, as observed between 40 and 60 s.

During the pyrolysis period from 60 to 80 s, the aromatic ring structures undergo rapid transition from guaiacol to catechol (2-hydroxyphenol), *o*-cresol (2-methylphenol) and phenol types, along with an increase in the total yield of the GC/MS-detectable products. These changes result from homolytic cleavage of the side chain C–C bonds of the condensation products as well as from reactions of methoxyl groups, as discussed in Sect. 11.5. In this stage, the unsaturated side chains are almost completely replaced by saturated alkyl groups (methyl, ethyl and propyl). Dealkylation through the addition of hydrogen radicals to the aromatic

rings also proceeds. These events are all associated with the secondary pyrolysis stage at the DTG temperature in the vicinity of 450 °C (Fig. 11.1).

The yields of catechol-type products rapidly diminish between 80 and 120 s (corresponding to the DTG peak at 550–600 °C), at which point the ring-opening of the catechol rings to form non-condensable gases such as CO takes place, as discussed in Sect. 11.5. Polyaromatic hydrocarbons (PAHs), including naphthalene, fluorene, phenanthrene and anthracene, also start to form over this temperature range.

On the basis of the above, it is evident that the pyrolysis temperature is a very important factor determining the chemical composition of the volatile products obtained from lignins. It can also be seen that the product compositions are reasonably explained on the basis of primary and secondary pyrolysis reactions.

11.4 Primary Pyrolysis Reactions

As noted, lignin is a heterogeneous polymer including various ether and condensed type linkages between phenylpropane units. As an example, spruce (a softwood) MWL is reported to include 63–67% ether linkages (such as 48% β-ether and 11.5–15% α-ether) and 30–35% condensed linkages (including 9.5–11% 5-5′ [biphenyl] and 9–12% β-aryl) [1]. The proportions of ether linkages in hardwood lignins including S and G units are normally higher than those of the softwood lignins, as can be seen from the 60% β-ether linkage proportion in birch (a hardwood) MWL [1]. Accordingly, the roles of these linkages (or substructures) during pyrolysis in the temperature range of 200–400 °C are quite important with regard to understanding the primary pyrolysis step of lignins.

In this section, the reaction mechanisms involved in the primary pyrolysis step are described, based on data obtained using model compounds.

11.4.1 Model Compound Reactivity

The use of model dimers that represent the lignin ether and condensed type linkages is an effective means of understanding the pyrolytic reactions of lignins having heterogeneous chemical structures. Figure 11.3 summarizes the degradation pathways of various phenolic (Ph) and non-phenolic (Non-ph) model dimers during treatment at 400 °C in an open-top reactor [10]. The model phenolic dimers represent the end groups of lignin macromolecules, while the non-phenolic dimers represent the repeating units. This system allows the pyrolysis products to quickly escape from the heated zone, thus favoring primary reactions over secondary ones. As discussed in Sect. 11.4.4, the primary pyrolysis products from lignins are normally quite unstable even at temperatures lower than their formation temperatures.

Biphenyl (5-5′) dimers in both the phenolic and non-phenolic compounds are quite stable, even at 400 °C. The non-phenolic β-aryl dimer tends to undergo

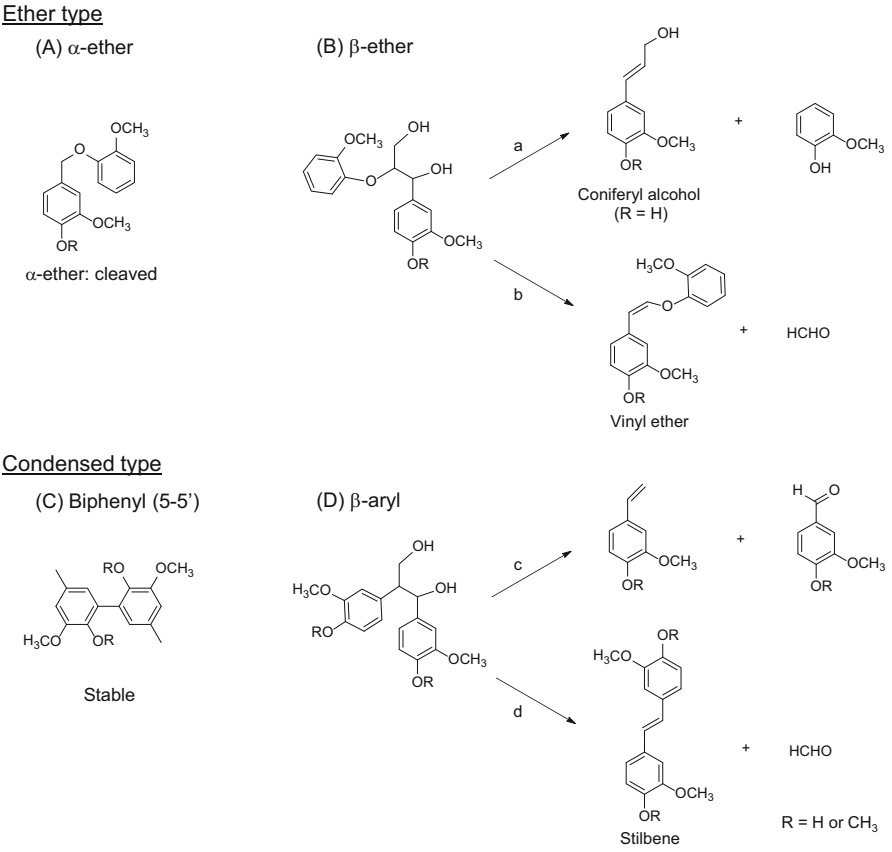

Fig. 11.3 Degradation pathways of ether and condensed linkage lignin model dimers under N_2 following immersion in a salt bath preheated to 400 °C for 1 min (Adapted with permission from Ref. [10], Copyright © 2007 Springer)

transition to a stilbene along with the fragmentation products formed through the cleavage of C_α–C_β bonds. The latter reaction leads to the depolymerization of the lignin macromolecule, although this reaction proceeds minimally even at 400 °C. The phenolic β-aryl dimer is very reactive and selectively generates a stilbene in approximately 50 mol% yield. Because stilbenes are formed through the elimination of the side chain (C_γ), the contributions of condensed linkages appear to be very limited during the pyrolytic depolymerization of lignin macromolecules.

Conversely, the ether linkages are cleaved quite effectively at 400 °C, a process that contributes to lignin depolymerization. The α-ether dimers were cleaved effectively, although this was followed by re-polymerization to form higher MW products. The β-ether dimer in phenolic form (guaiacylglycerol-β-guaiacyl ether) gave coniferyl alcohol in a 30.4 mol% yield, representing 60 mol% of the decomposition products of this dimer. Accordingly, the phenolic β-ether structures must be cleaved

to selectively form cinnamyl alcohols, such as coniferyl alcohol from the G lignin. Interestingly, these are the monomers that are utilized in lignin biosynthesis during the cell wall lignification process [31]. As discussed in Sect. 11.4.4, coniferyl alcohol is further degraded into various substances, including condensation products. Elimination of the C_γ-carbon, likely as formaldehyde, also proceeds to give vinyl ether, as observed in the formation of stilbenes from the β-aryl dimers. These results contradict those of an earlier study by Brežný et al. [7], which reported a complex mixture of products from the same β-ether dimers. This difference might have resulted from the use of a closed type reactor in the case of the earlier work, possibly allowing secondary reactions of the primary products to proceed. Consequently, the primary pyrolysis reactions of these substructures are evidently not as complicated as might be expected from the final pyrolysis product mixtures obtained from lignins.

The formation of coniferyl alcohol (from the β-ether structure) and stilbene (from the β-aryl structure) during the pyrolysis of natural lignins has also been confirmed by ultraviolet (UV) and IR spectroscopic analyses of the pyrolyzates of Japanese cedar MWL [11].

Phenolic dimers are normally more reactive than the corresponding non-phenolic dimers. As an example, the onset temperatures obtained during model dimer pyrolysis over a 1 min timespan are: α-ether (<200 °C [Ph], 350 °C [Non-ph]), β-ether (250–300 °C [Ph], 400 °C [Non-ph]) and β-aryl (300–350 °C [Ph], 400 °C [Non-ph]) [11]. Thus, the phenolic end groups in lignin macromolecules are expected to serve as reactive sites for the pyrolytic decomposition of lignins at relatively low temperatures. This is confirmed by the methylation of the phenolic hydroxyl groups of Japanese cedar MWL, which effectively inhibits pyrolytic conversion in the relatively low temperature region below 300 °C [11].

The TG data in Fig. 11.1 are evidence that Japanese cedar MWL undergoes efficient depolymerization at temperatures above the range of 300–350 °C (heating period: 1 min), even though the phenolic end-groups are expected to be reactive at lower temperatures based on the reactivities of the dimers and MWL described above. These apparently contradictory results can be explained by the repolymerization of the primary products generated by the depolymerization reactions (see Sect. 11.4.4). This is confirmed by the onset temperature range (300–350 °C) for the formation of the depolymerization products, a range that is not affected by the methylation of the hydroxyl groups in Japanese cedar MWL [11].

11.4.2 Ether Cleavage Mechanisms

Several heterolytic and homolytic mechanisms have been proposed for the pyrolytic cleavage of the β-ether bond, which is the most abundant linkage type in lignin macromolecules. With regard to heterolysis, Klein and Virk [9] proposed a six membered retro-ene mechanism based on an analysis of the kinetics of the formation of styrene and phenol from phenethyl phenyl ether, representing the simplest

model compound without any aromatic ring substituents or side chains. Brežný et al. [7] explained the pyrolysis products obtained from guaiacylglycerol-β-guaiacyl ether and its methylated derivative using an oxirane mechanism. Homolysis via C_α-radicals has also been suggested, based on the pyrolytic reactivity of phenethyl phenyl ether [32–34].

However, these mechanisms are not completely supported by reliable experimental evidence, and do not address the effects of aromatic ring substituent groups or side chains. As described above, the α- and β-ether bonds in phenolic dimers are cleaved at much lower temperatures than those in the corresponding non-phenolic dimers. In addition, elimination of the side chain hydroxyl groups significantly alters the reactivity for the cleavage of the β-ether bond in the phenolic form, as noted below in this section [35, 36]. Accordingly, the roles of such substituent groups must be explained when developing a complete set of molecular mechanisms.

It is helpful to study the effects of substituents on the cleavage reactivities of the α- and β-ether bonds in lignin model compounds, substituted at aromatic ring *para* positions, when elucidating the ether cleavage mechanisms (that is, heterolysis and homolysis) during pyrolysis [37]. The associated mechanisms are clearly indicated by plots of the cleavage reactivities against Hammett's substituent constant (σ_p) and against ΔBDE, a parameter that indicates the reduction in the bond dissociation energy (BDE) brought about by the substituent.

Assuming a heterolytic reaction, the ether linkage is cleaved to form a *para* substituted phenolate anion, and thus the reactivity should increase directly with the electron-attracting ability of the substituent group, as this stabilizes the anion. This property of the *para* position substituent may be quantified using Hammett's substituent constant, σ_p. Consequently, in the case of heterolysis, a positive correlation would be expected between cleavage reactivity and σ_p (Fig. 11.4).

In contrast, homolysis of the ether bond forms a phenoxy radical, and so the reactivity will vary depending on the stability of this species. When a stable radical is formed, cleavage of the ether linkage tends to proceed efficiently, because the increased stability of the radical reduces the BDE of the aromatic O–C bond. The stabilization obtained from a substituent is therefore reflected in the ΔBDE value. Thus, in the case of homolysis, a positive relationship is expected between reactivity and ΔBDE (Fig. 11.4). Fortunately, because the phenoxy radical is stabilized by electron donating substituents, σ_p, ΔBDE values tend to be increase in the opposite order: σ_p in the order of $-COCH_3 > -Cl > -H > -OCH_3$ and ΔBDE in the order of $-OCH_3 > -Cl > -H > -COCH_3$. Accordingly, the cleavage mechanism is clearly indicated by comparing plots of reactivities (the amounts of model compound reacted) against σ_p and ΔBDE.

Based on the substituent effects observed for α-ether type dimers with $-COCH_3$, –Cl, –H and $-OCH_3$ groups at the *para* positions of the C_α-phenoxyl group, the α-ether bond in the non-phenolic (methylated) form is confirmed to undergo homolytic cleavage (Fig. 11.5A) [37]. This is consistent with the relatively high temperature (350 °C) required for the cleavage of this bond. However, in the phenolic form, the substituent effects exhibit a heterolytic mechanism (Fig. 11.5B) [37]. The push

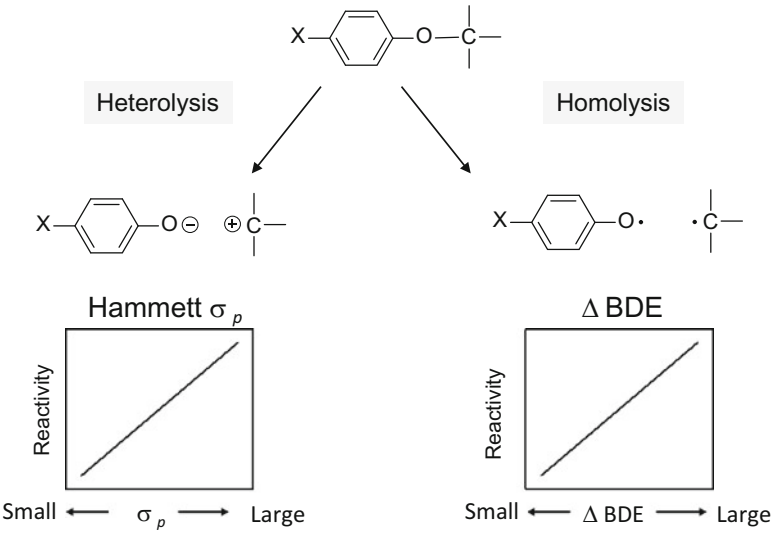

Fig. 11.4 Effect of the *para* substituent on the ether cleavage reactivity of lignin model compounds utilized for the elucidation of the ether cleavage mechanisms (heterolysis and homolysis) in pyrolysis. BDE: bond dissociation energy

and pull reaction that generates a quinone methide intermediate results in very efficient heterolysis of the C_α–O bond in the phenolic dimer. This reduces the cleavage temperature to <200 °C, significantly lower than the 350 °C required to cleave the non-phenolic α-ether bond, which cannot form a stable quinone methide intermediate.

The cleavage mechanisms associated with β-ether bonds are more complicated, because the reactivity varies depending on the side-chain hydroxylation pattern and the reactor type (see Sect. 11.4.3), as well as the use of phenolic or non-phenolic compounds.

Unexpectedly, the reactivity of a phenolic β-ether dimer was lowered to the level of a non-phenolic dimer by eliminating one of the hydroxyl groups from the C_α and C_γ of the guaiacylglycerol-β-guaiacyl ether [35, 36]. The effect of eliminating the C_α–OH is attributed to the inhibition of quinone methide formation, as illustrated in Fig. 11.5C. Low temperature homolysis of the C_β–O bond via a quinone methide intermediate during aqueous phase delignification [38–40] and steam-explosion [41] conditions has previously been postulated. Ponomarev [42] calculated the BDE of the C_β–O bond in the quinone methide form to be 44.1 kcal/mol, a value that is much lower than that of the phenolic form (57.0 kcal/mol). The reactivity for the cleavage of the β-ether bond of guaiacylglycerol-β-guaiacyl ether is not affected by the addition of tetralin as a radical scavenger, indicating that the rate-determining step is not the homolysis of the C_β–O bond but rather the formation of the quinone methide via a heterolysis reaction [43].

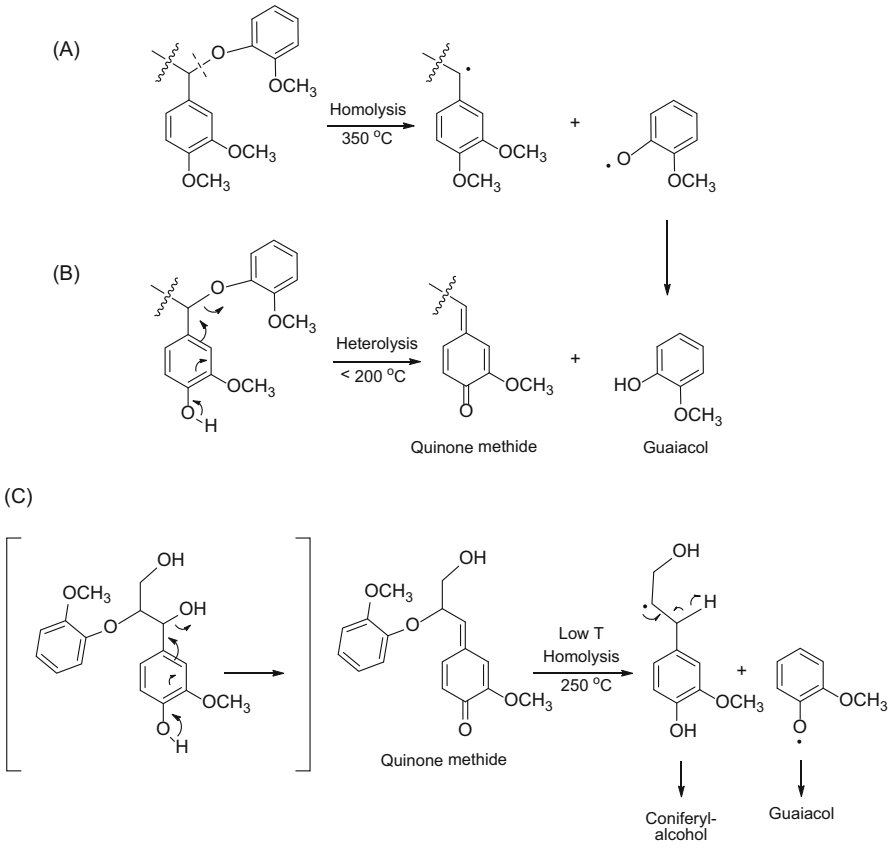

Fig. 11.5 Ether cleavage mechanisms proposed for the α- and β-ethers in lignins

The role of the quinone methide intermediate in the cleavage of the C_β–O bond in the phenolic end group can also be deduced from the reactivities of phenolic α,β-diether trimers that include various substituents at the *para* positions of the C_α-phenoxyl groups [37]. The reactivities of the β-ether bonds depend solely on those of the α-ether bonds, demonstrating that the cleavage of the α-ether bond acts as the rate-determining step. As noted, the α-ether bond in phenolic compounds is cleaved heterolytically to form the quinone methide intermediate. Furthermore, the substituent effect observed for a trimer incorporating a $–OCH_3$ group, which has a large ΔBDE value, are changed to those associated with a homolytic mechanism for the α-ether bond in the α,β-diether-type trimer. Radical species produced by the homolytic cleavage of the β-ether bond of the quinone methide intermediate would be expected to abstract hydrogen from the phenolic hydroxyl group. The resulting phenoxy radical would subsequently cleave the α-ether linkage in the trimer through β-scission to form the quinone methide intermediate (see Sect. 11.4.3, Fig. 11.6 pathway a).

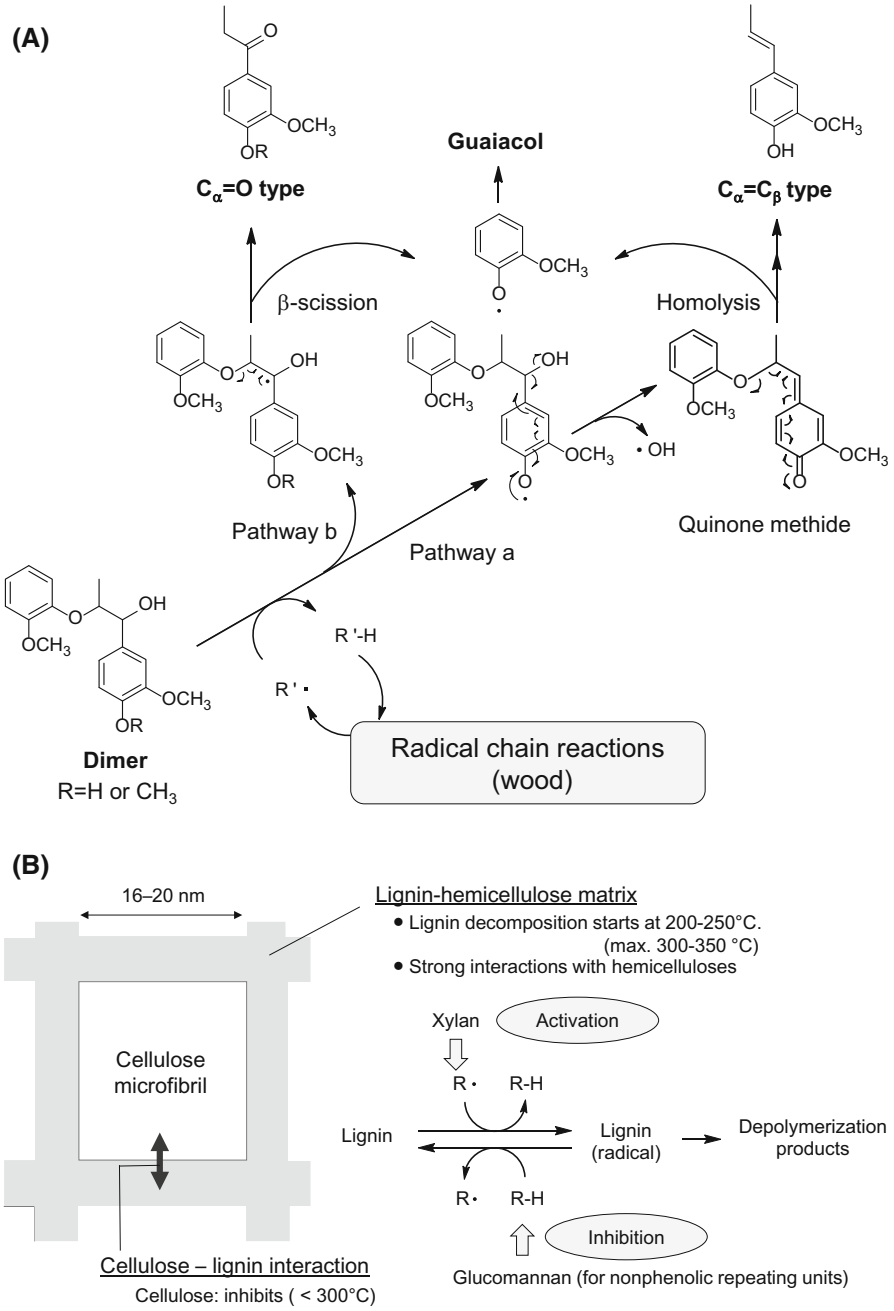

Fig. 11.6 (**a**) Summary of *in situ* method for studying the radical chain reactions of lignin using model dimers and (**b**) the interactions indicated between the constituent polymers of the cell wall, suggesting strong interactions between lignin and hemicellulose/cellulose (Adapted with permission from Ref. [44], Copyright © 2015 Elsevier)

During the pyrolysis of a non-phenolic α,β-diether trimer, the cleavage of the α-ether bond also serves as the rate-determining step for the scission of the β-ether bond. A β-scission type reaction with the C_α–radical, formed by the homolytic cleavage of the C_α–O bond, simultaneously cleaves the C_β–O bond homolytically [37].

The unexpected role of the C_γ–OH group of guaiacylglycerol-β-guaiacyl ether is explained by the stabilization effect on the transition state of the quinone methide formation (a heterolytic reaction) [35, 36]. Although the details of the mechanism are not known, hydrogen bonding between the C_α and C_γ hydroxyl groups may stabilize the transition state, promoting the elimination of the hydroxyl group from the C_α under pyrolysis conditions without requiring any stabilization effects via solvation. Similar stabilization effects have been proposed to explain the higher reactivities of β-hydroxy ketones compared with other ketones during retro-aldol condensation [45]. Intermolecular hydrogen bonding, which acts as an acid catalyst, is also a key factor in activating the transglycosylation and dehydration reactions during the molten phase pyrolysis of carbohydrates [46–48]. Accordingly, carbohydrates are quite stable in the gas phase, in which intermolecular hydrogen bonding is not important [49].

As discussed above, the heterolysis of the C_α–OR bonds is an important reaction that tends to accelerate the homolytic cleavage of the β-ether linkage via the quinone methide intermediate. However, the unexpected effects of C_γ–OH groups on the formation of the quinone methide suggest that the heterolysis of the C_α–OR bonds is greatly affected by the three-dimensional structure of the lignin. The DTG peak temperature (approximately 350 °C) corresponding to the primary pyrolysis of Japanese cedar lignin suggests that cleavage of the β-ether linkages via the quinone methide mechanism, as observed for dimers and trimers, does not proceed very efficiently in lignins [11].

The β-ether linkages of the non-phenolic dimers are comparatively stable, even at 400 °C in an open-top reactor, although the reactivity increases in a sealed reactor (see Sect. 11.4.3). Direct homolysis of the C_β–O bonds are clearly indicated based on the substituent effects of non-phenolic β-ether dimers substituted in varying manners at the *para* positions of the C_β-phenoxyl groups (–H, $–OCH_3$, –Cl) [43].

Based on this evidence, the majority of the ether linkages between phenylpropane units are considered to be cleaved homolytically, except for the α-ether bonds in the phenolic end groups. This process leads to the formation of a large number of radical species during the primary devolatilization step. It is important to consider this new information, especially when assessing the interactions between lignin and cellulose/hemicellulose during pyrolysis, because the volatile products from cellulose and hemicellulose are non-radical species, generated through the heterolytic cleavage of glycosidic C–O bonds [47, 48].

11.4.3 Radical Chain Reactions

It has been suggested that radical chain reactions take place during the pyrolytic devolatilization of lignins during the primary pyrolysis stage. This is evident from the reactivities of the C_γ–deoxy β-ether dimers that vary substantially depending on the reactor type [43]. To avoid any uncertainty arising from the effects of the C_γ–OH groups on the formation of the quinone methide when working with phenolic model dimers, C_γ–deoxy type dimers are frequently employed for the investigation of radical chain reactions. Many papers also have reported radical chain mechanisms for the pyrolytic cleavage of phenethyl phenyl ether and its derivatives [32–34].

In the case of an open-top reactor, which allows volatile products to readily exit the heated zone, the majority of phenolic and non-phenolic dimers can be recovered without undergoing pyrolysis reactions. However, the reactivities of these compounds are dramatically increased in a sealed reactor, especially that of the phenolic dimers, giving β-ether cleavage products, including isoeugenol and 4-*O*-methyl isoeugenol from phenolic and non-phenolic (methylated) dimers, respectively [43]. These compounds correspond to coniferyl alcohol and its methyl ether derivative, as obtained from C_γ–OH type dimers. Furthermore, the addition of tetralin as a radical scavenger has been shown to effectively suppress the reactivities, such that the level of reactivity becomes comparable to that in an open-top reactor at a tetralin/dimer ratio of 20 (mol/mol) [43]. These observations clearly indicate that radical chain reactions occur in a sealed reactor.

Based on analyses of the pyrolyzates from C_γ – deoxy dimers, the two pathways shown in Fig. 11.6 are believed to be involved in the radical chain reactions [50]. One path proceeds via the phenoxy radical formed by the abstraction of hydrogen from the phenolic hydroxyl group, which is further converted to the quinone methide intermediate through a β-scission type reaction. The C_β–O bond is subsequently cleaved to give isoeugenol (pathway a). The alternate pathway (b) proceeds via the C_α–radical, which further fragments into a C_α=O type monomer along with guaiacol through a β-scission reaction. These pathways have been confirmed by studying kinetic deuterium isotope effects during the formation of these products from regiospecifically deuterated dimers [51].

It was noted in the previous section that the C_α–O linkage (representing a benzyl ether) in lignin α-ether structures is least resistant to homolysis. Accordingly, the role of this bond in the radical chain reactions has also been investigated, using an α,β-diether trimer [1-(4-(3,4-dimethoxybenzoyloxy)-3-methoxyphenyl)-2-(2-methoxyphenoxy)-1-propanol] representing the benzyl ether derivative (R: $-CH_2-C_6H_5$) of the model dimer in Fig. 11.6. This trimer (320 °C) exhibited reactivity intermediate between those of the phenolic (260 °C) and non-phenolic (methylated, 360 °C) dimers, where the values in parentheses indicate the onset temperature of pyrolytic decomposition in a sealed reactor over a heating period of 2 min [50]. The higher reactivity of the trimer relative to the methylated dimer can be explainable by considering the homolysis of the C_α–O bond of the trimer as an initial step.

The extremely high reactivity of the phenolic dimer, which does not include any bonds that readily undergo homolysis, can be attributed to the formation of three radicals from the phenoxy radical intermediate through the homolytic cleavage of the C_β–O bond and the quinone methide formation (pathway a in Fig. 11.6) [50]. In contrast, the number of radical species does not change in pathway b because the C_α–radical is fragmented into one radical and one non-radical species. Thus, radical coupling reactions may terminate the chain reactions, as suggested by the formation of C-benzylated products from the pyrolyzates of the α,β-diether-type trimer [50]. These species are formed from the coupling of benzyl radicals and aromatic C radicals as a result of rearrangements of the phenoxy radical.

Consequently, the phenolic end-groups are expected to act as radical sensitizers in native lignin pyrolysis. As such, adding the phenolic dimer increases the reactivity of the non-phenolic dimers, while that of the phenolic dimer is decreased. This results in the pyrolytic decomposition of the two species taking place over essentially the same temperature region (between 300 and 400 °C), which is close to the DTG peak temperature (350 °C) corresponding to the primary pyrolysis of Japanese cedar lignin [51].

This model dimer system has also been applied to the investigation of the interactions of lignin with hemicellulose and cellulose in plant cell walls [44]. The cell walls in wood samples (with thicknesses of 1–10 μm) consist of heterogeneous layered structures, in which cellulose microfibrils (16–20 nm across) are filled with a matrix consisting of hemicellulose and lignin [52]. Accordingly, the heterogeneous nature of the wood cell wall structure should be considered when assessing the pyrolysis reactions of wood constituent polymers, including lignins. Lignins in this matrix will undergo pyrolysis while being affected by the pyrolysis of hemicellulose. Lignins are also expected to be pyrolyzed differently in softwoods and hardwoods, because these woods have different hemicellulose compositions; xylan is the major hemicellulose in hardwoods, while glucomannan accounts for the majority in softwoods.

To allow for the study of radical chain reactions of lignins in wood and other lignocellulosic biomass resources, an *in situ* dimer probe method has been developed, based on the changes in the reactivity of dimers in the presence of wood and its constituent polymers (MWL, hemicelluloses [xylan or glucomannan] and cellulose) [44]. As shown in Fig. 11.6, phenolic and non-phenolic dimers having similar chemical structures to native lignins can be utilized as models of the terminal phenolic and non-phenolic repeating phenylpropane units in lignins, respectively. It is also possible to follow the pyrolysis reactions (that is, the radical chain reactions) of dimers under the influence of co-existing substances by assessing the chemical compositions of the dimer-derived products.

The radical chain reactions (pathways a and b) responsible for the cleavage of the β-ether linkages in lignins begin in the temperature range of 200–250 °C, in which the pure dimers are stable, and become particularly frequent in the range of 300–350 °C [44]. This is consistent with the DTG peak temperature (350 °C) corresponding to the primary pyrolysis of Japanese cedar lignin.

Strong interactions between lignin and wood polysaccharides are indicated based on the significant effects of wood polysaccharides on the reactivity of dimers, which are also dependent on the type of polysaccharide and the pyrolysis temperature [44]. Two different types of hemicellulose exhibit very different effects on the reactivity; xylan activates the radical chain reactions of dimers, whereas glucomannan strongly inhibits the non-phenolic dimer. Based on these results, depolymerization of the lignin via radical chain reactions is expected to occur more effectively in hardwoods than in softwoods. This hypothesis is supported by the results obtained from studies of Japanese cedar wood (a softwood) and Japanese beech wood (a hardwood) [6].

The effect of cellulose is greatly dependent on the pyrolysis temperature [44]. Cellulose inhibits the radical chain reactions of lignins at temperatures below 300 °C, although these effects are minimal at temperatures above 350 °C, at which cellulose rapidly decomposes. Taking into account the heterogeneous nature of the cell wall structure, these interactions are expected to occur at the boundary surfaces between the cellulose microfibrils and the lignin-hemicellulose matrix.

11.4.4 Re-polymerization and Side Chain Conversion

As discussed in the previous sections, cinnamyl alcohols such as coniferyl alcohol are believed to be the most important primary products in lignin pyrolysis, and are formed from the cleavage of the β-ether bonds in lignins. In contrast, the contributions of cinnamyl alcohols in the pyrolyzates from wood and isolated lignins are much smaller than expected from studies using model compounds. Coniferyl aldehyde, isoeugenol, dihydroconiferyl alcohol, 4-vinylguaiacol and vanillin have been reported as more important products from the pyrolysis of G-lignin. Only direct mass spectrometric analysis of the pyrolyzates from wood and lignin samples without cooling indicates the significant contributions of coniferyl alcohol (MW: 180) and sinapyl alcohol (MW: 210), based on intense peaks observed at *m/z* 180 and 210 [53]. These apparently contradictory observations arise from the propensity of coniferyl alcohol and sinapyl alcohol to undergo secondary reactions, especially condensation (polymerization). Once cooled to an oily state, the pyrolyzates (including these compounds) do not subsequently evaporate completely. In addition, even at temperatures (<300 °C) lower than those used for pyrolysis, secondary reactions of these compounds have been found to occur quite efficiently.

The evaporation and degradation of *trans*-coniferyl alcohol and other monomeric products have been studied using an open-top reactor system made of a Pyrex glass tube (internal diameter 8.0 mm, length 300 mm) under nitrogen [54]. After the heat treatment of a small amount (5.0 mg) of coniferyl alcohol added to the bottom of the reactor, the reactor wall was sectioned approximately 1.5 cm from the bottom of the reactor to produce two regions. The compounds recovered from the upper part of the reactor wall represented the volatile substances that are evaporated from the bottom section. Using this system, the evaporation of coniferyl alcohol, which competes with the secondary reactions, was studied over the temperature range of

200–350 °C, a range that is lower than the DTG peak temperature (350 °C) corresponding to the primary pyrolysis of Japanese cedar lignin.

The evaporation and degradation of coniferyl alcohol were determined to start at 200 to 250 °C (heating period: 5 min), and polymerization was found to be a more important process than the evaporation and side chain conversion processes [54]. Coniferyl aldehyde (**2**, R: –CH=CH–CHO) (an oxidation product), dihydroconiferyl alcohol (**3**, R: $–CH_2–CH_2–CH_2OH$) and isoeugenol (**4**, R: $–CH=CH–CH_3$) (reduction products) were all formed as side chain conversion products, together with *cis*-coniferyl alcohol and 4-vinylguaiacol (**5**, R: $–CH=CH_2$) (Fig. 11.7). Accordingly, some redox reactions evidently take place during the pyrolysis of coniferyl alcohol (see Sect. 11.4.5). Furthermore, these products are quite similar to the pyrolyzates obtained from the pyrolysis of Japanese cedar wood and MWL under similar conditions [55]. This finding supports the hypothesis that guaiacols with various side chains are formed via coniferyl alcohol during the pyrolysis of lignins.

Nevertheless, the total yields of compounds **2**–**5** were less than 15 wt% of the coniferyl alcohol used for the experiment, although these yields increased with an increase in the pyrolysis temperature (Fig. 11.7). The evaporation efficiency of the coniferyl alcohol (**1**) also directly increased with the pyrolysis temperature, although the levels were only approximately 15% at 300 and 350 °C, at which point the coniferyl alcohol recovered from the bottom of the reactor wall was negligible.

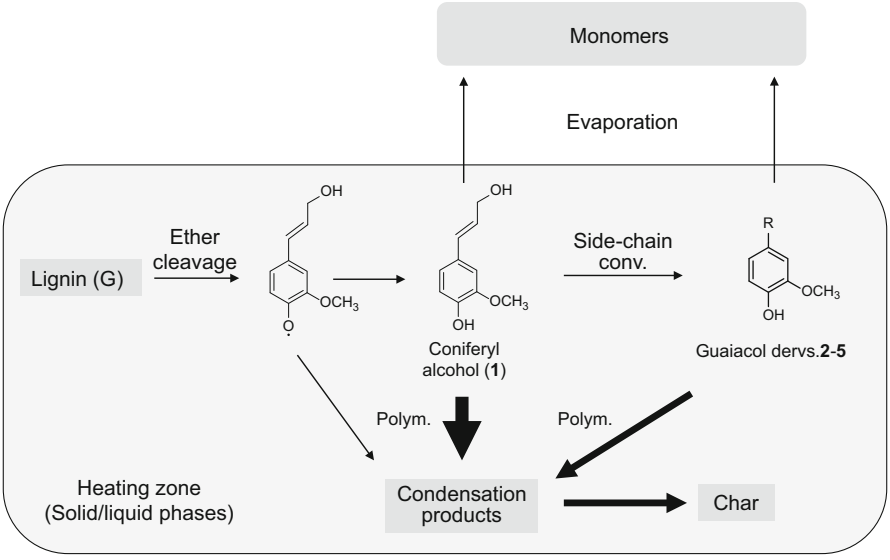

Fig. 11.7 Primary pyrolysis step, including depolymerization of the lignin macromolecule through ether cleavage, followed by two competing processes: evaporation of the monomeric products and re-polymerization to condensation products and char (Adapted with permission from Ref. [54], Copyright © 2014 Elsevier and [55], Copyright © 2013 Elsevier)

Based on the results of gel permeation chromatographic (GPC) analyses of the pyrolyzates, the remainder of the yield (approximately 70%) was found to consist of polymerization products. These results suggest that the coniferyl alcohol yield is low even when it is formed during the pyrolysis of G-type lignin.

The evaporation and polymerization behavior of compounds **2**–**5**, evaluated with a similar experimental system, demonstrate that **2**, **4** and **5**, all bearing conjugated C_α=C_β structures, were also prone to polymerization, although the reactivities for polymerization were much lower than that of coniferyl alcohol [54]. Because compound **3**, which does not contain a conjugated double bond, was selectively evaporated before condensation, the presence of conjugated C_α=C_β bonds is evidently the key to polymerization.

Methylation of the phenolic hydroxyl group of coniferyl alcohol (**1**) significantly suppresses the condensation reactivity [54, 56], although methylation does not alter the polymerization reactivity of 4-vinylguaiacol (**5**) [56]. From the chemical structure of the dimeric product obtained from **5**, a radical chain vinyl condensation mechanism has been proposed for the polymerization of 4-vinylguaiacol and its methyl ether derivative [56]. In the case of coniferyl alcohol, the bulky C_γ–hydroxymethyl group is believed to suppress the vinyl condensation reactivity.

Although a dimer fraction could not be isolated from the pyrolyzates of coniferyl alcohol at 250 °C, pyrolysis in the presence of creosol (4-methylguaiacol) gave two dimers (**6** and **7**, Fig. 11.8) [56]. Based on these results, a quinone methide mechanism can be proposed for the thermal condensation of coniferyl alcohol. Similar mechanisms have also been considered for the polymerization of coniferyl aldehyde (**2**) and isoeugenol (**4**). The reactivities for quinone methide formation from the guaiacol derivatives with conjugated C_α=C_β units are much more efficient than those of compounds with C_α–OR groups, which are the original structures observed in natural lignins. For these reasons, the primary pyrolysis products are more reactive for thermal polymerization than are natural lignins.

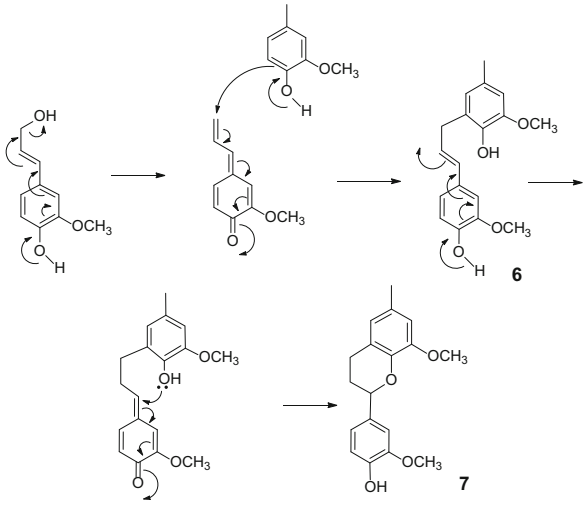

Fig. 11.8 Mechanisms for the condensation of coniferyl alcohol with 4-methylguaiacol through reactive quinone methide intermediates as a proposed explanation for the condensation products **6** and **7** obtained at 250 °C

The compound 4-*O*-methyl coniferyl alcohol is relatively stable against thermal polymerization although, in the presence of coniferyl alcohol, this compound was incorporated into the condensation process of coniferyl alcohol [54]. This result provides some insight into the pyrolysis of natural lignins, showing that coniferyl alcohol structures can also add to the repeating phenylpropane units.

Sinapyl alcohol, the corresponding primary product from S-type lignins, exhibits similar reactions to those observed for coniferyl alcohol, except for the radical sensitivity at a relatively high pyrolysis temperature of 350 °C [57], as discussed below.

11.4.5 Side-Chain Conversion Mechanism

The mechanisms proposed for the formation of *cis*-coniferyl alcohol (**1**), coniferyl aldehyde (**2**), dihydroconiferyl alcohol (**3**), isoeugenol (**4**), and 4-vinylguaiacol (**5**) are shown in Fig. 11.9 [54]. These mechanisms include the quinone methide (A) and radical chain (B) pathways.

Isomerization from trans to cis coniferyl alcohol is possible via both quinone methide intermediate A (pathway a) and C_α- and C_γ-radicals (pathways d and e). Higher trans/cis ratios are usually observed during pyrolysis, with the equilibrium tending towards the more stable trans isomer for steric reasons.

Coniferyl aldehyde (**2**) would be formed via the C_γ-radical intermediate (pathway c). Two pathways are considered for the formation of this radical intermediate, involving either homolytic cleavage of the C_γ–H bond or hydrogen abstraction (H-abstraction) from the C_γ–H bond by a radical species. The relatively large calculated BDE (79.9 kcal/mol, density functional theory (DFT)/B3LYP/6-311+G**) suggests that the later H-abstraction pathway is more probable. The β-scission-type reaction from the C_γ-radical would give a coniferyl aldehyde and a hydrogen radical (H-radical). This H-radical could be used for addition to a double bond and hydrogen donation (H-donation) to stabilize other radical species.

Dihydroconiferyl alcohol (**3**) is a hydrogenation product of coniferyl alcohol. The direct addition of a H-radical to the double bond of coniferyl alcohol (pathways d and e) and hydrogenation to form quinone methide intermediate A (pathway a) are both plausible reaction pathways. 4-*O*-Methyl coniferyl alcohol also gives a dihydroconiferyl alcohol type derivative, which indicates that direct H-radical addition pathways d and e are involved in this transformation. Formation of a H-radical would be necessary for both pathways. Formation of this type of compound could therefore be used as a probe for the H-radical in the pyrolysis environment, as well as formation of isoeugenol.

Both the quinone methide (pathway b) and radical (pathway e) mechanisms are considered for the formation of isoeugenol (**4**) from coniferyl alcohol. Quinone methide intermediate B formed by elimination of the hydroxy group from the C_γ atom of coniferyl alcohol would be hydrogenated. In the radical mechanism, elimination of the C_γ-hydroxy group could proceed in two different ways: by β-scission-type elimination of the OH radical from the C_β-radical intermediate or by direct

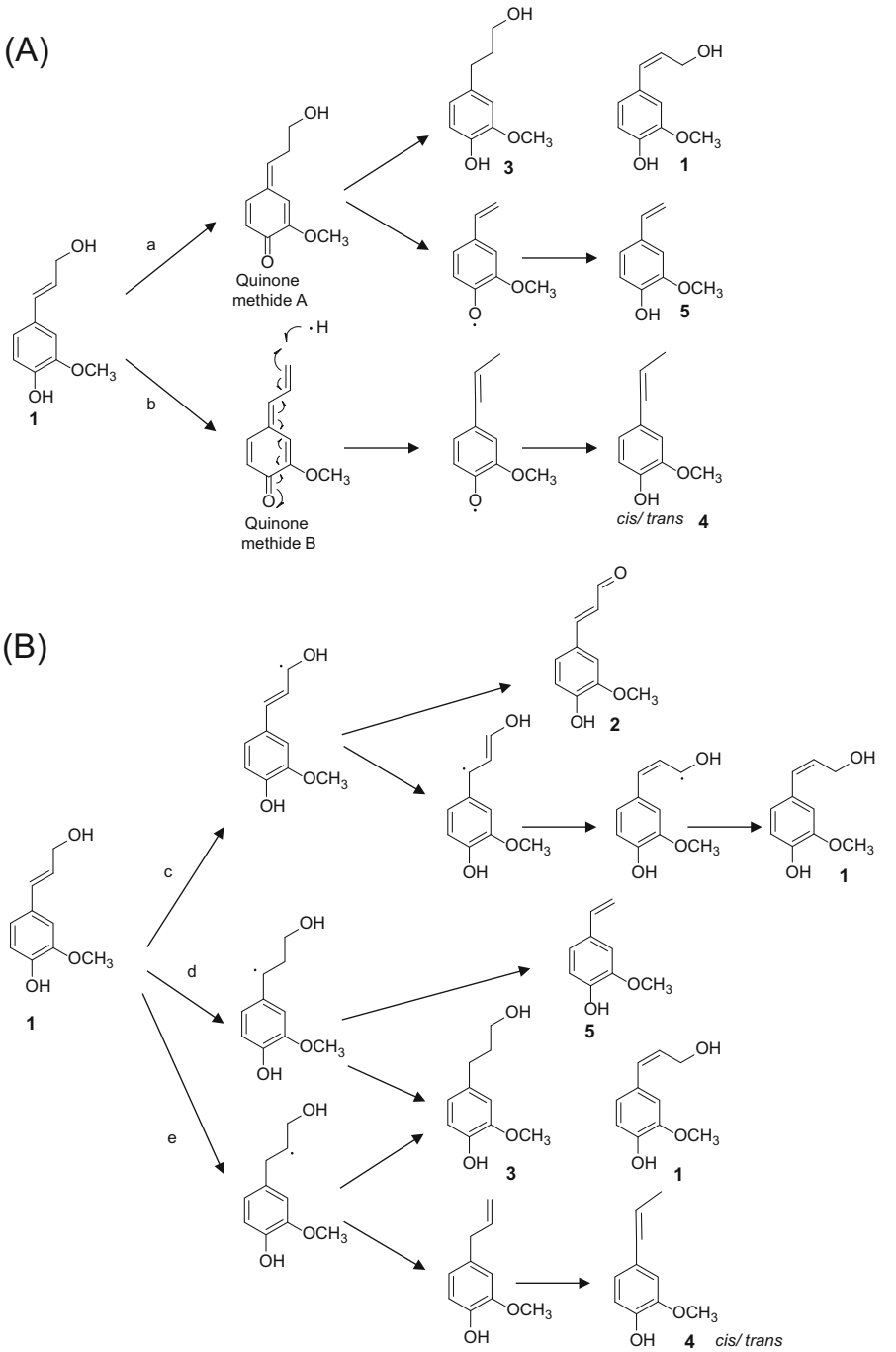

Fig. 11.9 Side-chain conversion mechanisms of coniferyl alcohol in the temperature range 200–350 °C to give compounds **2**–**5** (Adapted with permission from Ref. [54], Copyright © 2013 Elsevier)

homolysis of the C_γ–OH bond. However, the calculated BDE (72.2 kcal/mol, DFT/B3LYP/6-311+G**) would be too large for the homolysis pathway at pyrolysis temperature less than 350 °C. The C_β-radical pathway would therefore be more probable. In a manner analogous to the dihydroconiferyl alcohol formation mechanism, formation of the isoeugenol-type structure from 4-*O*-methyl coniferyl alcohol suggests that pathway e is involved in this conversion process.

4-Vinylguaiacol (**5**) would be formed via C_α-radical (pathway d) and quinone methide intermediate A (pathway a). Homolytic C_β–C_γ bond cleavage of the quinone methide intermediate A would occur. The electron-withdrawing quinone methide moieties attached to the C_β positions would reduce the BDE of the C_β–C_γ bonds to 51.8 kcal/mol (DFT/B3LYP/6-311+G**). Formation of this type of products from 4-*O*-methyl coniferyl alcohol suggests that radical pathway d is involved in the formation of **5**.

11.4.6 Role of Cinnamyl Alcohol in Lignin Primary Pyrolysis

The roles of the characteristic features of coniferyl alcohol and sinapyl alcohol in lignin pyrolysis have been carefully investigated using Japanese cedar, Japanese beech, and their MWL fractions in the temperature range 250–350 °C [55, 57]. As described above, the product compositions from wood and MWL samples are similar to those from pyrolysis of coniferyl alcohol and sinapyl alcohol. Because large parts of the lignin ether linkages are homolytically cleaved, the influences of diphenoxybenzene (DPB) (an aprotic solvent) and 1,2,3,10b-tetrahydrofluoranthene (a hydrogen donor, H-donor) on the monomer formation are different for wood/MWL and coniferyl alcohol/sinapyl alcohol [55, 57]. The following discussion mainly focuses on G-type lignin [55].

Pyrolysis in DPB is very effective to increase the recovery of coniferyl alcohol during pyrolysis of coniferyl alcohol by suppression of thermal polymerization [55]. This is probably because of inhibition of proton-transfer, which is as an important step in formation of quinone methide intermediates (heterolysis reaction).

In contrast to coniferyl alcohol, both DPB and H-donors are required for effective formation of the monomer from lignin contained in Japanese cedar and the MWL fraction [55]. Such differences can be explained by stabilization of the coniferyl alcohol radical with the H-donor as a primary product from homolytic cleavage of the β-ether linkages in lignin (Fig. 11.7). The amount of H-donor is usually not sufficient to stabilize all of the radical species formed through cleavage of ether linkages. Under these conditions, primary radicals tend to undergo radical coupling reactions. For pyrolysis in DPB containing a H-donor, the yields of monomeric guaiacols reach 8.3 and 12.8 wt% (lignin-based) from MWL and wood samples, respectively, and the side-chain reduction products (dihydroconiferyl alcohol and isoeugenol) are the main components of the monomers. These are produced by addition of a H-radical (from H-donor thermal decomposition) to the C=C double bond of the side-chain of coniferyl alcohol.

The polymer effect is also suggested to promote the secondary reactions of lignin primary pyrolyzates [55]. Cleavage of the ether linkages at the terminal end-groups of the lignin macromolecule leads to direct formation of monomers. This is similar to the pyrolysis reactions of coniferyl alcohol and model dimers. In contrast, the secondary reactions proceeded more effectively in pyrolysis of MWL/wood. Cleavage of ether linkages within the polymer would not lead to immediate formation of monomers from lignin because of its polymeric nature. In these circumstances, pyrolyzates would remain in the heating zone and undergo secondary reactions prior to the formation of monomers through cleavage of their ether linkages. These polymer effects would reduce the monomer yield and increase the contributions of the side-chain conversion products, including compounds **2–5**.

In pyrolysis of MWL/wood, the relative efficiency of oxidation/reduction of the side-chain of coniferyl alcohol varies depending on the pyrolysis temperature [55]. At the relatively low temperature of 250 °C, coniferyl aldehyde (**2**), an oxidation product, is the main monomer from lignin. This can be explained by the H-donor/radical balance. During the early stage of primary pyrolysis of lignin, the pyrolysis environment is considered to be under radical conditions through homolytic cleavage of lignin ether linkages. Under such H-donor-deficient conditions, these radical species would tend to condense or abstract hydrogen atoms from other molecules. The C_γ-hydrogen atom of coniferyl alcohol, which is at the conjugated allyl position, would be the site of H-abstraction, and this abstraction leads to production of coniferyl aldehyde (Fig. 11.9). In contrast, at a relatively high pyrolysis temperature of 350 °C, the pyrolysis environment would be richer in H-donor species (H-radicals). H-radicals are formed during charring reactions, which effectively promote pyrolytic radical chain reactions of guaiacol and syringol [30] (see Sect. 11.5.1). The presence of high levels of H-donor (H-radical) species would increase the monomer yield and the selectivity for side-chain reduction products, such as dihydroconiferyl alcohol (**3**) and isoeugenol (**4**).

Oligomeric products should also be considered as initial products along with monomers, because condensed (C–C) linkages are stable during primary pyrolysis of lignin [55]. Consequently, the monomer yield is estimated to be as low as ∼30% from a schematic softwood lignin structure composed of 16 C9 units, even without considering secondary polymerization. The rest of the products should be obtained as oligomeric products with relatively low volatilities, which preferentially condense under neat conditions. The use of DPB and H-donors significantly increases the yields of oligomers, as observed for monomer formation from lignin.

In summary (Fig. 11.7), two competitive reactions (i.e., H-addition and the radical coupling reaction to form condensation products) occur for the coniferyl alcohol radical following its formation during primary pyrolysis of lignin (DTG peak temperature ∼350 °C). This temperature would be sufficiently high to cause the secondary reaction of coniferyl alcohol. Although evaporation and the secondary degradation process are competitive under such conditions, the most important reaction is the condensation reaction, followed by side-chain conversion reactions. The relative efficiencies of the evaporation/polymerization/side-chain conversion

processes would determine the yield of monomeric products and their composition.

For condensation of coniferyl alcohol, the quinone methide intermediate is an important intermediate. The electropositive carbon atoms of quinone methides tend to react with electronegative aromatic and double-bonded carbon atoms rather than with oxygen atoms of the side-chain and phenolic groups. This reactivity can be explained by the hard and soft acid and base rule. Given that condensed (C–C) linkages are much more stable than ether linkages during the lignin pyrolysis process, re-depolymerization would not be effective for the condensation products. Together with the high condensation reactivity of the primary products, this would explain why lignin pyrolysis tends to preferentially form solid products (char).

Concerning the role of sinapyl alcohol in the pyrolysis of S-type lignins, analogous to coniferyl alcohol, sinapyl alcohol preferentially gives condensation products, along with similar side-chain conversion products [57]. The formation behavior of monomeric guaiacols and syringols from pyrolysis of Japanese beech wood and the MWL fraction can be explained by the reactivities of coniferyl alcohol and sinapyl alcohol as the pyrolysis intermediates formed as radical species. Remarkable differences are only observed for the evaporation efficiency and radical sensitivity of sinapyl alcohol [57].

The recovery of sinapyl alcohol (expected boiling point 385 °C) by evaporation is lower than that of coniferyl alcohol (expected boiling point 332 °C), most likely because of its low evaporation efficiency compared with the condensation reactivity [57]. Pyrolysis of sinapyl alcohol in DPB increases the recovery of sinapyl alcohol at 250 and 300 °C by suppression of the condensation reactivity. However, unlike coniferyl alcohol pyrolysis, DPB is insufficient to increase the recovery at 350 °C, and the additional use of a H-donor is required to increase the monomeric syringol recovery [57]. Based on these results, it is suggested that sinapyl alcohol is more susceptible to free radical reactions than coniferyl alcohol at 350 °C. These results also suggest that formation of monomeric syringols is less effective than monomeric guaiacols.

Although addition of a H-donor significantly increases the monomer yields from Japanese cedar wood (a softwood) and its MWL fraction, the influence on pyrolysis of Japanese beech wood (a hardwood) is very limited, and relatively large amounts of monomers are produced even without addition of any H-donors [57]. Based on these results, we proposed that pyrolysis of other wood constituents (probably hemicellulose) of beech wood acts as a source of H-donors and H-radicals to stabilize the intermediate radicals. Together with activation of lignin radical chain reactions by pyrolysis of xylan (Sect. 11.4.3, Fig. 11.6), these results indicate the different influences of softwood and hardwood hemicelluloses.

11.5 Secondary Reactions

As shown in Fig. 11.10, by increasing the pyrolysis temperature to ~450 °C, methoxyl groups attached to the lignin aromatic rings become very reactive for homolytic cleavage of the O–CH_3 bond. Radical-induced rearrangement of the methoxyl group also simultaneously occurs. Owing to these reactions, the aromatic substituent changes from –OCH_3 to –OH and –CH_3. Demethoxylation also proceeds via the formyl intermediate during the rearrangement pathway, along with formation of coke, a solid carbonized substance formed from volatile products.

When the pyrolysis temperature is further increased to 550–600 °C, formation of PAHs, demethylation of the aromatic moiety, and decomposition of catechols and pyrogarolls into non-condensable gases (mainly CO) occurs.

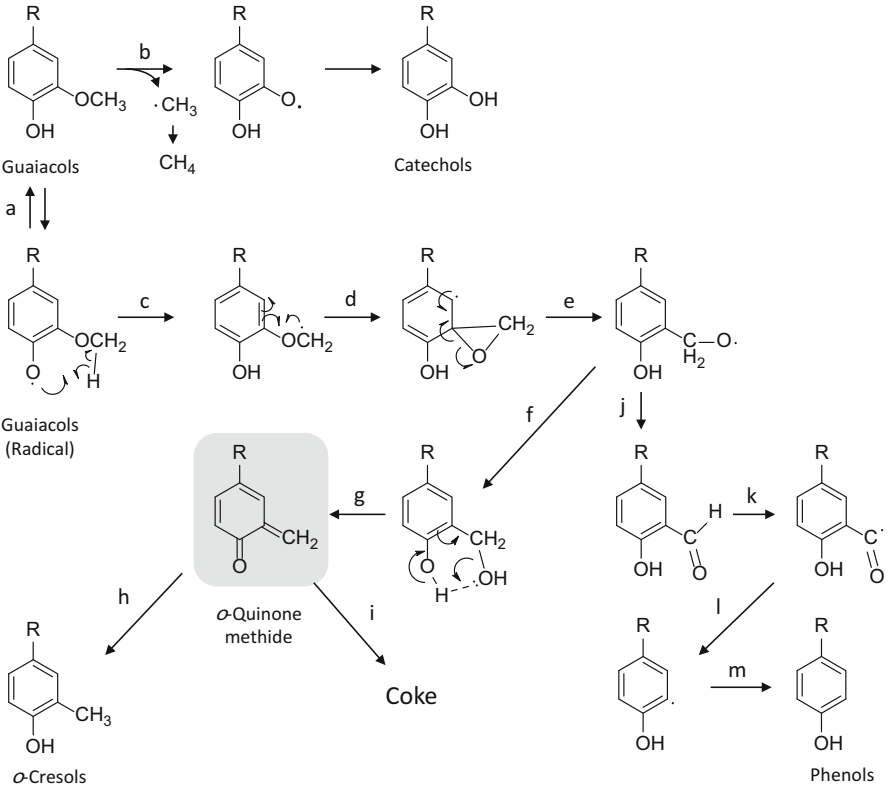

Fig. 11.10 Conversion mechanisms of guaiacol-type aromatic rings to catechols, *o*-cresols, and phenols, which proceed effectively at pyrolysis temperatures higher than 450 °C

11.5.1 Homolysis and Rearrangement of Methoxyl Groups

H-Abstraction and H-donation play important roles in the homolysis and rearrangement pathways. Catechol and methyl radicals formed by homolysis reaction b are stabilized by formation of catechol and methane, respectively, when two H-donors can donate hydrogen atoms to these radicals. Otherwise, these radicals would be consumed by radical coupling reactions. Methylation of aromatic rings by coupling of the methyl radical and C-centered radicals formed as resonance structures of phenoxy radicals also occurs [30].

The rearrangement pathway starts from the phenoxy radical of guaiacol [58], which is formed by H-abstraction from the phenolic hydroxyl group of guaiacol. Intramolecular H-abstraction at the methyl group by the phenoxy radical (reaction c) and subsequent 1,2-aryl migration (reaction e) have been proposed for the ether-rearrangement mechanism [58, 59]. This type of 1,2-aryl migration is supported by the high-yield formation of *o*-hydroxybenzaldehyde (reaction j) from guaiacol in the presence of cumene (a H-donor) [58]. This 1,2-aryl migration product is further converted into *o*-quinone methide (reaction g, a key intermediate) [60, 61], which is subsequently hydrogenated to *o*-cresol (reaction h).

Demethoxylation occurs by α-scission of the formyl radical (reaction l) formed by H-abstraction from *o*-hydroxybenzaldehyde (reaction k) [30, 58]. This type of reaction converts syringols formed as primary pyrolysis products of S-type lignins to guaiacols and finally phenols [30].

These pathways would be influenced by the concentrations of H-acceptors (radicals) and H-donors [62]. For catechol/CH_4 formation, only H-donors are required, because catechol and methyl radicals are supplied by unimolecular decomposition of guaiacol (O–CH_3 bond homolysis). In contrast, formation of other products by the OCH_3 rearrangement pathway starting from the guaiacol radical requires both H-acceptors and H-donors. The numbers of H-acceptors/H-donors required for formation of *o*-quinone methide, *o*-cresol, and phenol from guaiacol are 1/1, 1/3, and 3/1, respectively. Accordingly, the selectivity for the homolysis and rearrangement pathways can be controlled by changing the concentrations of H-acceptors/H-donors in the pyrolysis environment [63] (see Sect. 11.5.5).

Asmadi et al. [62] suggested that polyaromatization during the charring reaction activates the pyrolysis reactions in Fig. 11.10 by acting as a source of H-radicals, which can act as both H-acceptors and H-donors. A combination of guaiacol and syringol markedly suppressed coking in an ampoule reactor (N_2/600 °C/40–600 s), although the mechanism of the mixing effect is unknown. This also reduced the O–CH_3 bond homolysis products in the early stage of pyrolysis, while it enhanced the formation of condensation products. This can be explained by the decrease in the concentration of the H-donor stabilizing phenoxy radicals. To confirm this hypothesis, pyrolysis of the guaiacol/syringol mixture was performed in the presence of guaiacol coke, which drastically enhanced most of the products in Fig. 11.10.

Stereoelectronic effects are known for H-donation to radical species because all of the intermediates favor a linear transition state, which maximizes the interaction

between the radical orbital and the vacant σ* orbital of the bond that is going to be cleaved. H-donation by a small H-radical would be effective for steric reasons.

From the S-type lignin in Japanese beech wood, pyrogallol, 3-methoxycatechol, 3-methylcatechol, and 2,6-xylenol are produced as O–CH_3 bond homolysis and rearrangement products via syringol primary pyrolysis products [30]. 2,6-Xylenol is also produced from the G-type lignin by coupling of *o*-cresol with methyl radicals, and other pyrogallol and catechol derivatives disappear because of gasification, as discussed in Sect. 11.5.4. Accordingly, the lignin-derived products are different only in the primary pyrolysis stage, while the compositions for S- and G-type lignins are similar after the secondary reactions [30, 64].

11.5.2 Coke and Polyaromatic Hydrocarbon Formation

Coke and PAH formation are important because of the tar problem in biomass gasification. Issues related to tar formation represent a challenge that must be overcome to allow establishment of reliable gasification systems. Tar causes clogging of the pipeline from the outlet of the gasifier and can damage engines and turbines used for power generation by condensing and coking on walls.

The coke formation behavior of volatiles formed during the primary pyrolysis stage is different for lignin and polysaccharides [65]. In pyrolysis of wood polysaccharides, coking primarily occurs by condensation of volatile intermediates on the reactor wall at lower temperatures. Thus, cooling of volatile intermediates during gasification would lead to clogging of the pipeline from the gasifier. This stability of polysaccharide-derived volatiles in the gas phase has been explained by intermolecular hydrogen bonding, which can act as an acid catalyst only in the liquid (molten) phase to promote liquid-phase reactions leading to polymerization and dehydration to form coke [49, 65–67]. These reactions have been extensively studied using levoglucosan (1,6-anhydro-β-D-glucopyranose) as the important intermediate of cellulose pyrolysis along with other low MW glycosides [47–49, 67, 68]. In contrast, volatiles from lignin are subject to vapor-phase reactions that continuously produce coke materials from the bottom, where lignin is placed for pyrolysis, to the top of the reactor wall.

Coking of lignin-derived volatile intermediates has been suggested to be closely related to the *o*-quinone methide intermediate formed by rearrangement of the OCH_3 group (Fig. 11.10). Hosoya et al. [69] compared the coking behavior of various types of pyrolysis products with guaiacol-, cresol-, catechol- and phenol-type aromatic nuclei. They found that only guaiacols with methoxyl groups exhibited high reactivities for coke formation (in closed ampoule/N_2/600 °C/80 s, the final temperature reached 569 °C). Interestingly, the ethoxyl group was not effective in such coke formation. 2-Ethoxyphenol gave 2,3-benzofuran rather than formation of coke. This can be reasonably explained by the different reactivities of the *o*-quinone methide intermediates: the *o*-quinone methide intermediate formed from 2-ethoxyphenol has a reactive allyl moiety, which tends to be converted to

2,3-benzofuran by addition of the allyl radical formed by H-abstraction to the carbonyl oxygen of the *o*-quinone methide intermediate. The coking mechanism for the *o*-quinone methide intermediate (Fig. 11.10, reaction i) is not clear, although Diels–Alder type reactions proceed to form 9*H*-xanthene and its derivatives with OH/CH_3. Similar reactions are also expected in char formation, although the details are not known.

Even though the reactivities of cresols/xylenols and catechols/pyrogallols are much lower than those of guaiacols (in closed ampoule/N_2/600 °C), they also give coke substances by increasing the pyrolysis period and temperature to 600 s and 600 °C [70]. Thus, coking reactions of guaiacols/syringols occur in two stages: guaiacols/syringols with methoxyl groups simultaneously give coke during rearrangement of the methoxyl group, while coke formation from cresols/xylenols and catechols/pyrogallols occurs at higher pyrolysis temperatures. The same *o*-quinone methide intermediate can be formed from *o*-cresol by abstraction of phenolic and benzylic hydrogen atoms. It should be noted that the coke yield increases with increasing number of methyl groups: *o*-cresol (6.1 wt%) < 2,4-xylenol (12.8 wt%), 2,6-xylenol (9.2 wt%) < 2,4,6-trimethylphenol (23.5 wt%) (in closed ampoule/N_2/600 °C) [70]. Phenol and 2-ethylphenol do not form any coke materials. Therefore, methoxyl and methyl groups are the key structural elements for coke formation.

At the stage where cresols/xylenols and catechols/pyrogallols become reactive for coke formation, PAHs start to form from guaiacol/syringol via their pyrolysis products, which include biphenyl and naphthalene (two aromatic rings), and phenanthrene and anthracene (three aromatic rings) at temperatures up to 600 °C [6, 30, 64]. There are many papers that deal with PAH formation by thermal decomposition of catechol and phenol at much higher temperatures [71–74]. Reactive intermediates such as the cyclopentadienyl radical formed by decomposition of aromatic rings are considered to be involved in PAH formation.

Regarding the reactivities of guaiacol and syringol as the primary pyrolysis products from G- and S-type lignins, the most significant difference is observed in the first-stage coke yield, which is almost two times higher for syringol [30]. This effective coking can be explained by the influence of the additional OCH_3 group in syringol, which doubles the opportunity for coke formation. Consequently, the yields of GC/MS-detectable low MW products are two times higher for guaiacol than for syringol. Because the reactivities of cresols/xylenols and catechols/pyrogallols tend to be enhanced by increasing the number of substituent groups on phenol, syringol-derived intermediates are more reactive than the corresponding guaiacol-derived intermediates [70]. These characteristic features for the pyrolysis of guaiacol and syringol are confirmed by the pyrolysis of Japanese cedar, Japanese beech, and their MWL fractions [6, 64].

From the results of stepwise pyrolysis of the char and coke fractions from MWLs at 450 and 600 °C, methoxyl group-related reactions (Fig. 11.10) (450 °C) and intermediate gasification (600 °C) have been confirmed to occur in the solid/liquid phase [6]. In the case of solid/liquid-phase reactions, tar formation, especially catechols/pyrogallols and PAHs, is significantly suppressed. Thus, gas-phase secondary reactions would be a source of PAHs at 600 °C.

11.5.3 Dealkylation

Several papers have described the hydrogen-transfer reaction in the aromatic ring during coal liquefaction in H-donor solvents such as tetralin, which is followed by cleavage of the strong bond between the aromatic ring and the aliphatic side-chain [75, 76]. Lignin pyrolyzates obtained at the secondary reaction stage include methylated aromatic compounds such as cresols and xylenols, which are formed by OCH_3 rearrangement (Fig. 11.10), methylation by radical coupling with the methyl radical, and homolysis of C–C bonds in ethyl and propyl side-chains of the intermediates. These methylated phenols are subject to demethylation reactions [70, 77, 78].

Demethylation is the main reaction for cresols/xylenols at 600 °C along with coke formation (second stage) [70]. For pyrolysis of *o*-cresol and 2,6-xylenol at 600 °C (in ampoule/600 s), the total yields of the monomers formed by demethylation reach 18.0 and 18.2 wt%, respectively, although gas formation is very limited. Thus, *o*-cresol is converted to phenol, and 2,6-xylenol is converted to *o*-cresol.

The 2,3-xylenol selectively gives *m*-cresol (32.6 wt%) in preference to *o*-cresol (1.4 wt%) [70]. As indicated by this example, demethylation reactions proceed regioselectively and methyl groups at the *o*- and *p*-positions with respect to the phenolic hydroxyl group are selectively cleaved. The higher reactivities of the *o*- and *p*-methyl groups are explained by the following two mechanisms [70]. First, because of the relative stability of the intermediate cyclohexadienyl radicals formed by attack of the H-radical to the aromatic ring-carbons, the resonance structure with the radical on the carbon atom adjacent to the OH group stabilizes the radicals. The second proposed mechanism is based on radical coupling of C-centered radicals (selectively formed at the *o*- and *p*-positions) as resonance structures of phenoxy radicals with H-radicals. These coupling reactions lead to formation of cyclohexanedienones, which have weaker C–CH_3 bonds. The calculated BDEs of the *o*- and *p*-derivatives are 60.3 and 62.5 kcal/mol, respectively (DFT/B3LYP/6-311++G**), which are much lower than the BDEs of the corresponding phenols (110.5 and 108.7 kcal/mol). As described for low-temperature homolysis of the β-ether linkage of the quinone methide intermediate (Sect. 11.4.2), the strong electron-withdrawing ability of the conjugated carbonyl moiety significantly decreases the BDE of the C–CH_3 bond.

11.5.4 Gasification

Gasification reactivities of lignin-derived volatile and charred intermediates have been compared with those of cellulose-derived products at 600 °C in ampoule reactors under nitrogen [21]. The cellulose-derived volatile intermediates from primary pyrolysis are efficiently gasified to form CO-rich gas, while the gasification reactivity significantly decreases by converting to the coke and char materials. In contrast, lignin is much less reactive for gasification under these pyrolysis conditions at

600 °C. Interestingly, the gasification reactivity is not considerably different for the lignin-derived volatile and char/coke materials. This can be explained by the above description that similar secondary reactions proceed for both phases of the intermediates (Sect. 11.5.2).

Methane content is generally higher in the gas produced from lignin than in that produced from cellulose. This is related to O–CH_3 bond homolysis and demethylation, both of which proceed at the secondary reaction stage. Based on comparison of the gas yields from MWLs and guaiacol/syringol, gas formation at the primary pyrolysis stage is more pronounced for MWLs. Part of the lignin side-chain would be transformed to gaseous products, which is supported by formation of C6–C2 structures during the primary pyrolysis of lignins and model dimers.

From the pyrolysis reactivities of cresols/xylenols and catechols/pyrogallols as the intermediates converted from guaiacols/syringols at 600 °C, catechol- and pyrogallol-moieties are efficiently converted into gaseous products containing CO as the main component [70]. Pyrogallol derivatives tend to be more reactive than catechol derivatives and produced CO_2 as well as CO, although the mechanism is not well understood. Nevertheless, S-type lignin produces more CO_2 than G-type lignin.

Composition of the gaseous products formed from cresols/xylenols are different from that produced from catechols/pyrogallols, in addition to the lower gasification reactivities [70]. Cresols/xylenols tend to produce CH_4 and H_2 rather than CO and CO_2, along with demethylation products and coke. These gas compositions can be explained by the secondary reactions described in Sects. 11.5.2 and 11.5.3. Methane is the product of H-donation to the methyl radical formed during demethylation. The coking process would produce H-radicals during polyaromatization, which leads to formation of H_2. Accordingly, the CH_4 yield is related to the number of methyl groups in cresols/xylenols, where the yield increased in the order *o*-cresol (2.8 wt%) < 2,4-xylenol (5.9 wt%) and 2,6-xylenol (6.0 wt%) < 1,3,5-trimethylphenol (9.5 wt%). The H_2 yield also increased in this order because the coke yield varied in this order (see Sect. 11.5.2).

11.5.5 Interaction Between Lignin and Polysaccharide Pyrolysis

As discussed above, radical reactions play important roles in the primary and secondary reactions of lignins, while heterolysis reactions to form non-radical intermediates dominate in pyrolysis of the polysaccharide components of wood and other lignocellulosic biomass. These features cause significant interactions between the pyrolysis of lignin and polysaccharides.

Polysaccharide-derived pyrolysis intermediates stabilize the lignin-derived intermediate radicals produced by primary pyrolysis, which increases the yields of GC/MS-detectable monomers from lignin [63, 79]. This is accomplished by stabili-

zation of radical intermediates by H-donation from polysaccharide-derived non-radical intermediates, probably aldehydes and other reactive hydrogen atoms in the molecules. Consequently, the secondary reactions are accelerated for the polysaccharide-derived intermediates (products). For example, conversion of anhydrosugars (including levoglucosan, an important intermediate in cellulose pyrolysis) to C2 and C3 fragmentation products is enhanced under the influence of lignin pyrolysis [63].

Anhydrosugars such as levoglucosan efficiently polymerize into polysaccharides by converting the vapor into a molten substance under cooling [49, 66]. This polymerization reaction is suppressed in the presence of lignin-derived products [68, 79]. This can be explained by general hydrogen-bonding theory, in which intermolecular hydrogen bonding acts as an acid catalyst. Hydrogen bonding between aromatic π-electrons and OH groups of anhydrosugars inhibits intermolecular hydrogen bonding between anhydrosugars. Consequently, both yields of anhydrosugar and C2/C3 fragments from cellulose increase in the presence of lignin pyrolysis, while the water-soluble polysaccharide yield decreases [79].

By increasing the pyrolysis temperature to >450 °C, coexisting polysaccharide pyrolysis significantly increases the selectivity for O–CH_3 bond homolysis products (i.e., catechols/pyrogallols and CH_4) over OCH_3 rearrangement products (e.g., cresols/xylenols and coke) [63]. For example, the yield of GC/MS-detectable monomers from Japanese cedar MWL increased from 5.3 to 20.2 wt% because of the influence of cellulose pyrolysis, and the selectivity of catechols over cresols/xylenols also increased from 0.9 to 5.5. These results are reasonably explained by the roles of H-acceptors and H-donors, as described in the discussion relating to the pathways in Fig. 11.10. Cellulose-derived intermediates, which can act as H-donors, suppress the OCH_3 rearrangement pathway by inhibiting formation of the phenoxy radical, which is the key intermediate in this pathway. This enhances conversion of cellulose-derived intermediates to gaseous products.

11.6 Conclusions and Future Outlook

The chemical structures of lignin are more complex than the polysaccharide components in lignocellulosic biomass because of the heterogeneity arising from the existence of several linkage types between the phenylpropane units in lignin. Although investigations using model dimers, which represent lignin linkage types, have clarified the molecular mechanisms underlying primary and secondary pyrolysis of lignin, many uncertainties still remain to be clarified, which include the influences of conformational mobility of lignin macromolecules, types of aromatic ring substitution patterns, minerals, other co-existing substances such as hemicellulose. Uncovering the molecular mechanisms of lignin and other components in lignocellulosic biomass would help to improve the existing thermochemical conversion processes for production of biofuels and biochemical.

References

1. Adler E. Lignin chemistry – past, present and future. Wood Sci Technol. 1977;11(3):169–218.
2. Fenner RA, Lephardt JO. Examination of the thermal-decomposition of kraft pine lignin by fourier-transform infrared evolved gas-analysis. J Agric Food Chem. 1981;29(4):846–9.
3. Gardner DJ, Schultz TP, McGinnis GD. The pyrolytic behavior of selected lignin preparations. J Wood Chem Technol. 1985;5(1):85–110.
4. Haw JF, Schultz TP. ^{13}C CP MAS NMR and FT-IR study of low-temperature lignin pyrolysis. Holzforschung. 1985;39(5):289–96.
5. Jakab E, Faix O, Till F. Thermal decomposition of milled wood lignins studied by thermogravimetry mass spectrometry. J Anal Appl Pyrolysis. 1997;40–1:171–86.
6. Asmadi M, Kawamoto H, Saka S. Gas- and solid/liquid-phase reactions during pyrolysis of softwood and hardwood lignins. J Anal Appl Pyrolysis. 2011;92(2):417–25.
7. Brežný R, Mihálov V, Kováčik V. Low-temperature thermolysis of lignin 1. Reactions of β-O-4 model compounds. Holzforschung. 1983;37(4):199–204.
8. Brežný R, Šurina I, Košik M. Low-temperature thermolysis of lignin 2. Thermofractography and thermal-analysis of β-O-4 model compounds. Holzforschung. 1984;38(1):19–24.
9. Klein MT, Virk PS. Model pathways in lignin thermolysis 1. Phenthyl phenyl ether. Ind Eng Chem Fund. 1983;22(1):35–45.
10. Kawamoto H, Horigoshi S, Saka S. Pyrolysis reactions of various lignin model dimers. J Wood Sci. 2007;53(2):168–74.
11. Nakamura T, Kawamoto H, Saka S. Pyrolysis behavior of Japanese cedar wood lignin studied with various model dimers. J Anal Appl Pyrolysis. 2008;81(2):173–82.
12. Faix O, Jakab E, Till F, Székely T. Study on low mass thermal-degradation products of milled wood lignins by thermogravimetry-mass-spectrometry. Wood Sci Technol. 1988;22(4):323–34.
13. Li J, Li B, Zhang X. Comparative studies of thermal degradation between larch lignin and manchurian ash lignin. Polym Degrad Stab. 2002;78:279–85.
14. Liu Q, Wang S, Zheng Y, Luo Z, Cen K. Mechanism study of wood lignin pyrolysis by using TG-FTIR analysis. J Anal Appl Pyrolysis. 2008;82(1):170–7.
15. Kuno S, Kadla J. Thermal decomposition study of isolated lignin using temperature modulated TGA. J Wood Chem Technol. 2008;28:106–21.
16. Sipilä K, Kuoppala E, Fagernäs L, Oasmaa A. Characterization of biomass-based flash pyrolysis oils. Biomass Bioenerg. 1998;14(2):103–13.
17. Branca C, Giudicianni P, Di Blasi C. GC/MS characterization of liquids generated from low-temperature pyrolysis of wood. Ind Eng Chem Res. 2003;42(14):3190–202.
18. Hosoya T, Kawamoto H, Saka S. Secondary reactions of lignin-derived primary tar components. J Anal Appl Pyrolysis. 2008;83(1):78–87.
19. Pindoria RV, Lim JY, Hawkes JE, Lazaro MJ, Herod AA, Kandiyoti R. Structural characterization of biomass pyrolysis tars/oils from eucalyptus wood waste: effect of H-2 pressure and sample configuration. Fuel. 1997;76(11):1013–23.
20. Sharma RK, Wooten JB, Baliga VL, Lin X, Geoffrey Chan W, Hajaligol MR. Characterization of chars from pyrolysis of lignin. Fuel. 2004;83(11–12):1469–82.
21. Hosoya T, Kawamoto H, Saka S. Pyrolysis gasification reactivities of primary tar and char fractions from cellulose and lignin as studied with a closed ampoule reactor. J Anal Appl Pyrolysis. 2008;83(1):71–7.
22. Dufour A, Castro-Diaz M, Brosse N, Bouroukba M, Snape C. The origin of molecular mobility during biomass pyrolysis as revealed by in situ ^{1}H NMR spectroscopy. ChemSusChem. 2012;5(7):1258–65.
23. Dufour A, Castro-Díaz M, Marchal P, Brosse N, Olcese R, Bouroukba M, et al. In situ analysis of biomass pyrolysis by high temperature rheology in relations with ^{1}H NMR. Energy Fuels. 2012;26(10):6432–41.

24. Scholze B, Meier D. Characterization of the water-insoluble fraction from pyrolysis oil (pyrolytic lignin). Part I. PY-GC/MS, FTIR, and functional groups. J Anal Appl Pyrolysis. 2001;60(1):41–54.
25. Genuit W, Boon JJ, Faix O. Characterization of beech milled wood lignin by pyrolysis-gas chromatography photoionization mass-spectrometry. Anal Chem. 1987;59(3):508–13.
26. Ralph J, Hatfield RD. Pyrolysis-Gc-Ms characterization of forage materials. J Agric Food Chem. 1991;39(8):1426–37.
27. Arias ME, Polvillo O, Rodríguez J, Hernández M, González-Pérez JA, González-Vila FJ. Thermal transformations of pine wood components under pyrolysis/gas chromatography/mass spectrometry conditions. J Anal Appl Pyrolysis. 2006;77(1):63–7.
28. Greenwood PF, van Heemst JDH, Guthrie EA, Hatcher PG. Laser micropyrolysis GC-MS of lignin. J Anal Appl Pyrolysis. 2002;62(2):365–73.
29. Alen R, Kuoppala E, Oesch P. Formation of the main degradation compound groups from wood and its components during pyrolysis. J Anal Appl Pyrolysis. 1996;36(2):137–48.
30. Asmadi M, Kawamoto H, Saka S. Thermal reactions of guaiacol and syringol as lignin model aromatic nuclei. J Anal Appl Pyrolysis. 2011;92(1):88–98.
31. Higuchi T. Lignin biochemistry: biosynthesis and biodegradation. Wood Sci Technol. 1991;24(1):23–63.
32. Autrey ST, Alnajjar MS, Nelson DA, Franz JA. Absolute rate constants for the β-scission reaction of the 1-phenyl-2-phenoxypropyl radical – a model for radical reactions of lignin. J Org Chem. 1991;56(6):2197–202.
33. Britt PF, Buchanan AC, Malcolm EA. Thermolysis of phenethyl phenyl ether – a model for ether linkages in lignin and low-rank coal. J Org Chem. 1995;60(20):6523–36.
34. Beste A, Buchanan III AC, Britt PF, Hathorn BC, Harrison RJ. Kinetic analysis of the pyrolysis of phenethyl phenyl ether: computational prediction of alpha/beta-selectivities. J Phys Chem A. 2007;111(48):12118–26.
35. Kawamoto H, Horigoshi S, Saka S. Effects of side-chain hydroxyl groups on pyrolytic β-ether cleavage of phenolic lignin model dimer. J Wood Sci. 2006;53(3):268–71.
36. Kawamoto H, Saka S. Role of side-chain hydroxyl groups in pyrolytic reaction of phenolic β-ether type of lignin dimer. J Wood Chem Technol. 2007;27(2):113–20.
37. Kawamoto H, Nakamura T, Saka S. Pyrolytic cleavage mechanisms of lignin-ether linkages: a study on *p*-substituted dimers and trimers. Holzforschung. 2008;62(1):50–6.
38. Sano Y. Reactivity of β-O-4 linkages in lignin during solvolysis pulping – degradation of β-O-4 lignin model compounds. Mokuzai Gakkaishi. 1989;35(9):813–19.
39. Kishimoto T, Sano Y. Delignification mechanism during high-boiling solvent pulping – Part 2. Homolysis of guaiacylglycerol-β-guaiacyl ether. Holzforschung. 2002;56(6):623–31.
40. Li S, Lundquist K. Reactions of the β-aryl ether lignin model 1-(4-hydroxy-3-methoxyphenyl)-2-(2-methoxyphenoxy)-1-propanol on heating in aqueous solution. Holzforschung. 2001;55(3):296–301.
41. Tanahashi M, Karina M, Tamabuchi K, Higuchi T. Degradation mechanism of lignin accompanying steam explosions 1. Degradation products of lignin and β-O-4 lignin substructure model dimers. Mokuzai Gakkaishi. 1989;35(2):135–43.
42. Ponomarev DA. Formation of quinone methides: an alternative pathway of thermal degradation of some β-O-4-ethers as compounds modeling lignin. Russ J Appl Chem. 1997;70(5):824–6.
43. Kawamoto H, Ryoritani M, Saka S. Different pyrolytic cleavage mechanisms of β-ether bond depending on the side-chain structure of lignin dimers. J Anal Appl Pyrolysis. 2008;81(1):88–94.
44. Kawamoto H, Watanabe T, Saka S. Strong interactions during lignin pyrolysis in wood – a study by in situ probing of the radical chain reactions using model dimers. J Anal Appl Pyrolysis. 2015;113:630–7.
45. Smith GG, Yates BL. Pyrolysis studies 15. Thermal retrograde aldol condensation of β-hydroxy ketones. J Org Chem. 1965;30(6):2067–8.

46. Matsuoka S, Kawamoto H, Saka S. Retro-aldol-type fragmentation of reducing sugars preferentially occurring in polyether at high temperature: role of the ether oxygen as a base catalyst. J Anal Appl Pyrolysis. 2012;93:24–32.
47. Kawamoto H, Ueno Y, Saka S. Thermal reactivities of non-reducing sugars in polyether—role of intermolecular hydrogen bonding in pyrolysis. J Anal Appl Pyrolysis. 2013;103:287–92.
48. Kawamoto H, Hosoya T, Ueno Y, Shoji T, Saka S. Thermal stabilization and decomposition of simple glycosides in the presence of aromatic substances in closed ampoules: the role of OH center dot center dot center dot pi hydrogen bonding. J Anal Appl Pyrolysis. 2014;109:41–6.
49. Fukutome A, Kawamoto H, Saka S. Processes forming gas, tar, and coke in cellulose gasification from gas-phase reactions of levoglucosan as intermediate. ChemSusChem. 2015;8(13):2240–9.
50. Watanabe T, Kawamoto H, Saka S. Radical chain reactions in pyrolytic cleavage of the ether linkages of lignin model dimers and a trimer. Holzforschung. 2009;63(4):424–30.
51. Watanabe T, Kawamoto H, Saka S. Pyrolytic reactivities of deuterated β-ether-type lignin model dimers. J Anal Appl Pyrolysis. 2015;112:23–8.
52. Salmén L. Micromechanical understanding of the cell-wall structure. C R Biol. 2004;327(9–10):873–80.
53. Evans RJ, Milne TA. Molecular characterization of the pyrolysis of biomass. 1. Fundamentals. Energy Fuels. 1987;1(2):123–37.
54. Kotake T, Kawamoto H, Saka S. Pyrolysis reactions of coniferyl alcohol as a model of the primary structure formed during lignin pyrolysis. J Anal Appl Pyrolysis. 2013;104:573–84.
55. Kotake T, Kawamoto H, Saka S. Mechanisms for the formation of monomers and oligomers during the pyrolysis of a softwood lignin. J Anal Appl Pyrolysis. 2014;105:309–16.
56. Nakamura T, Kawamoto H, Saka S. Condensation reactions of some lignin related compounds at relatively low pyrolysis temperature. J Wood Chem Technol. 2007;27(2):121–33.
57. Kotake T, Kawamoto H, Saka S. Pyrolytic formation of monomers from hardwood lignin as studied from the reactivities of the primary products. J Anal Appl Pyrolysis. 2015;113:57–64.
58. Dorrestijn E, Mulder P. The radical-induced decomposition of 2-methoxyphenol. J Chem Soc Perkin Trans. 1999;2(4):777–80.
59. Vuori A. Pyrolysis studies of some simple coal related aromatic methyl ethers. Fuel. 1986;65(11):1575–83.
60. Dorrestijn E, Epema OJ, van Scheppingen WB, Mulder P. *o*-Quinone methide as a common intermediate in the pyrolysis of *o*-hydroxybenzyl alcohol, chroman and 1,4-benzodioxin. J Chem Soc Perkin Trans. 1998;2(5):1173–8.
61. Dorrestijn E, Pugin R, Nogales MVC, Mulder P. Thermal decomposition of chroman. Reactivity of *o*-quinone methide. J Org Chem. 1997;62(14):4804–10.
62. Asmadi M, Kawamoto H, Saka S. The effects of combining guaiacol and syringol on their pyrolysis. Holzforschung. 2012;66(3):323–30.
63. Hosoya T, Kawamoto H, Saka S. Solid/liquid- and vapor-phase interactions between cellulose- and lignin-derived pyrolysis products. J Anal Appl Pyrolysis. 2009;85(1–2):237–46.
64. Asmadi M, Kawamoto H, Saka S. Pyrolysis reactions of Japanese cedar and Japanese beech woods in a closed ampoule reactor. J Wood Sci. 2010;56(4):319–30.
65. Hosoya T, Kawamoto H, Saka S. Pyrolysis behaviors of wood and its constituent polymers at gasification temperature. J Anal Appl Pyrolysis. 2007;78(2):328–36.
66. Hosoya T, Kawamoto H, Saka S. Different pyrolytic pathways of levoglucosan in vapor- and liquid/solid-phases. J Anal Appl Pyrolysis. 2008;83(1):64–70.
67. Fukutome A, Kawamoto H, Saka S. Gas- and coke-forming reactivities of cellulose-derived tar components under nitrogen and oxygen/nitrogen. J Anal Appl Pyrolysis. 2014;108:98–108.
68. Hosoya T, Kawamoto H, Saka S. Thermal stabilization of levoglucosan in aromatic substances. Carbohydr Res. 2006;341(13):2293–7.
69. Hosoya T, Kawamoto H, Saka S. Role of methoxyl group in char formation from lignin-related compounds. J Anal Appl Pyrolysis. 2009;84(1):79–83.

70. Asmadi M, Kawamoto H, Saka S. Thermal reactivities of catechols/pyrogallols and cresols/xylenols as lignin pyrolysis intermediates. J Anal Appl Pyrolysis. 2011;92(1):76–87.
71. Ledesma EB, Marsh ND, Sandrowitz AK, Wornat MJ. An experimental study on the thermal decomposition of catechol. Proc Combust Inst. 2002;29:2299–306.
72. Lomnicki S, Truong H, Dellinger B. Mechanisms of product formation from the pyrolytic thermal degradation of catechol. Chemosphere. 2008;73(4):629–33.
73. Marsh ND, Ledesma EB, Sandrowitz AK, Wornat MJ. Yields of polycyclic aromatic hydrocarbons from the pyrolysis of catechol [ortho-dihydroxybenzene]: temperature and residence time effects. Energy Fuels. 2004;18(1):209–17.
74. Ledesma EB, Marsh ND, Sandrowitz AK, Wornat MJ. Global kinetic rate parameters for the formation of polycyclic aromatic hydrocarbons from the pyrolysis of catechol, a model compound representative of solid fuel moieties. Energy Fuels. 2002;16(6):1331–6.
75. McMillen DF, Malhotra R, Hum GP, Chang SJ. Hydrogen-transfer-promoted bond scission initiated by coal fragments. Energy Fuels. 1987;1(2):193–8.
76. McMillen DF, Malhotra R, Chang SJ, Ogier WC, Nigenda SE, Fleming RH. Mechanisms of hydrogen transfer and bond scission of strongly bonded coal structures in donor solvent systems. Fuel. 1987;66(12):1611–20.
77. Jones BW, Neuworth MB. Thermal cracking of alkyl phenols – mechanism of dealkylation. Ind Eng Chem. 1952;44(12):2872–6.
78. Buryan P. Thermal-decomposition of dimethylphenol. J Anal Appl Pyrolysis. 1991;22(1–2):83–93.
79. Hosoya T, Kawamoto H, Saka S. Cellulose–hemicellulose and cellulose–lignin interactions in wood pyrolysis at gasification temperature. J Anal Appl Pyrolysis. 2007;80(1):118–25.